A Small DC-Link Capacitor Inverter Fed by Front-End Three-Phase Diode Rectifiers Used to Control Induction Motor

Ashwini V. Potdar and Ch. Mallareddy

Abstract This paper contains an approach to applications of a three-phase variable speed drive to improve power density as well as reliability by using small film capacitor inverter-based induction motor control. A performance by the electrolytic capacitor is very poor for the inverter fed by front-end diode rectifiers intercepted by motor controller which is compounded and strong in nature. The controller is designed with a hexagon voltage manipulating controller (HVC) and with composition of a model-based controller (MBC). The work of MBC and HVC together gives an output. MBC gives the command output voltage with losses of rotor flux with bisection of the torque. The enjoin voltage vector is set on simply by the requirement of torque command and the inverter which has a hexagon-shaped voltage boundary in the HVC mode. Prosperous utilization of the control proceed towards is supported by a Mathematically and graphically measure that normally head to a single voltage selection rule. The paper discovers the performance reactivity is very sensible to accumulation of motor parameter to sort out how to remove unwanted AC distortion or oscillations with state filter design.

Keywords Hexagon voltage manipulating controller (HVC) · Model-based controller (MBC) · Small film capacitor inverter · Front-end diode rectifiers

1 Introduction

The HVAC system is low-cost application of speed drive which is a variable; in this diode, rectifiers are generally used as the front-end circuit for higher reliability [1]. As shown in Fig. 1, three-phase diode rectifier and PWM inverter for IM drive electrolytic capacitors are generally used to balance time-to-time base i/p and o/p power and also voltage spike suppression occurred by operation of switching and

---

A. V. Potdar (✉)
Punysholk Ahilydevi Holkar Solapur University, Solapur, India

Ch. Mallareddy
FTCOER, Sangola, Solapur, India

H. S. Saini et al. (eds.), *Innovations in Electrical and Electronics Engineering*,
Lecture Notes in Electrical Engineering 626,
https://doi.org/10.1007/978-981-15-2256-7_3

leakage of inductance [2, 3]. And general study power electronics devices failed because of voltage spikes caused by parasitic lead of inductance.

Electrolytic capacitors are responsible for most of the breakdown according to the survey [4]. Therefore, for long time closed-loop current controller is used to regulating the air-gap torque and flux linkages in AC motors according to the studies [4–6].

2 Problem Statement

As shown in Fig. 1 as per given construction, DC-link voltage and o/p power to the motor decrease with the time because of the absence of energy storage device. So, the speed is decreased below base level and this leads to the problem of field weakening, anti-windup control and over-modulation. On the other hand, there is problem regarding utilization of voltage at extinct level because of circular voltage boundary.

3 Methodology

This paper gives the new idea about the position sensor-less vector controlled IM drive system integrated in HVAC system a Small DC link film fed by capacitor inverter a three-phase diode front-end diode rectifier is feeds power supply to motor.

Above-mentioned problems overcome by PI motor current regulator-free control strategy with combination of hexagon voltage manipulating controller (HVC). The MBC deals with the command output voltage with the intersection of torque and rotor flux linkage.

Figure 2 shows the idea about the various facts related to vectors. The MBC controls action at low speed, and HVC operates at high speed.

$$v_{ds_{\mathrm{HVC}}}^{e*} = \frac{B_n + \sqrt{B_n^2 - 4M_{n\gamma}}}{2M_n} \tag{1}$$

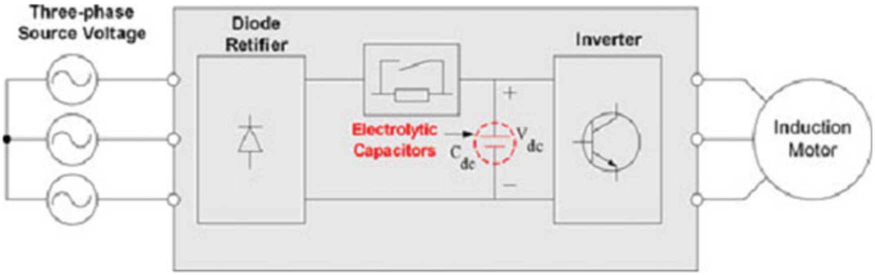

Fig. 1 Three-phase diode rectifier and PWM inverter for IM drive

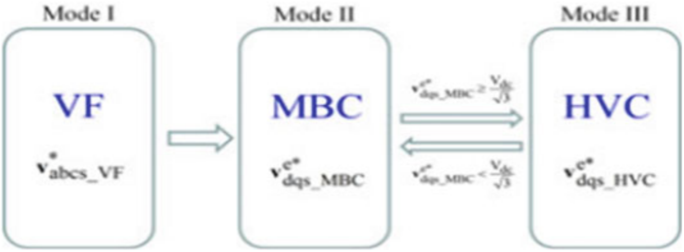

Fig. 2 Proposed IM control strategy for small capacitor inverters

$$v^{e*}_{qs_{\mathrm{HVC}}} = M_n \cdot v^{e*}_{ds_{\mathrm{HVC}}} + B_n \tag{2}$$

where

$$\gamma = \frac{T_e^*}{\frac{3}{2}\frac{P}{2}\frac{L_m^2}{L_r}\frac{1}{w_e^2 L_S \sigma L_s}}$$

$$v^{e*}_{ds}\text{\_MBC} = -w_e \sigma L_s \left(\frac{T_e^*}{\frac{3}{2}\frac{P}{2}\frac{L_m}{L_r}\lambda^{e*}_{dr}} \right) + R_s i^{e*}_{qs} \tag{3}$$

$$v^{e*}_{ds_{-\mathrm{MBC}}} = w_e L_s \frac{\lambda^{e*}_{dr}}{L_m} + R_s i^{e*}_{qs} \tag{4}$$

Equations 1, 2 deal with the hexagonal voltage boundary, and Eqs. 3, 4 deal with model-based controller which is shown in Figs. 3 and 4.

The motor torque is regulated around a desired torque line in the presence of rapid voltage variations.

Figure 4 shows the idea about the representations of stator voltage solutions between the torque curves and rotating hexagon, which bus shrinks the inverter DC bus voltage.

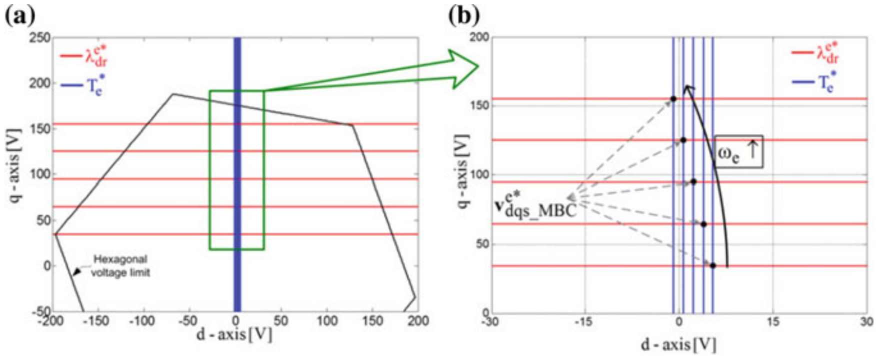

Fig. 3 Voltage command selection in the MBC mode

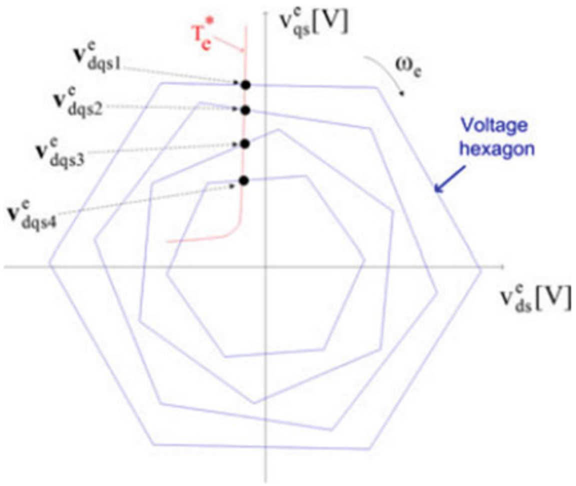

Fig. 4 Voltage command selection in the HVC mode

In this paper, we are replacing the electrolytic capacitor with the DC-link film capacitor, as well as design the state filter as shown in Fig. 5.

So, from the following simulation result we can compare between systems with different capacitors. From the following figures, we can calculate THD also, so the results are improved in terms of DC-link film capacitor.

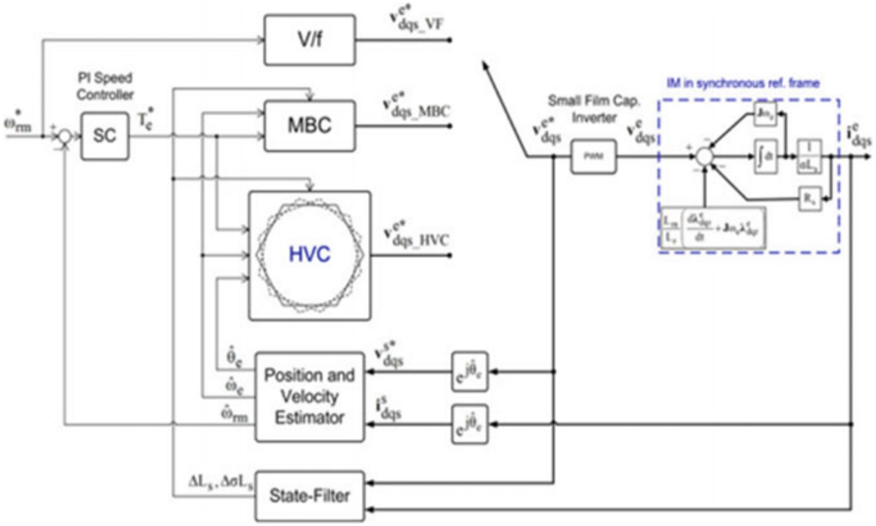

Fig. 5 Overall control block diagram

4 Result

4.1 Output Graph for Electrolytic Capacitor

See Fig. 6.

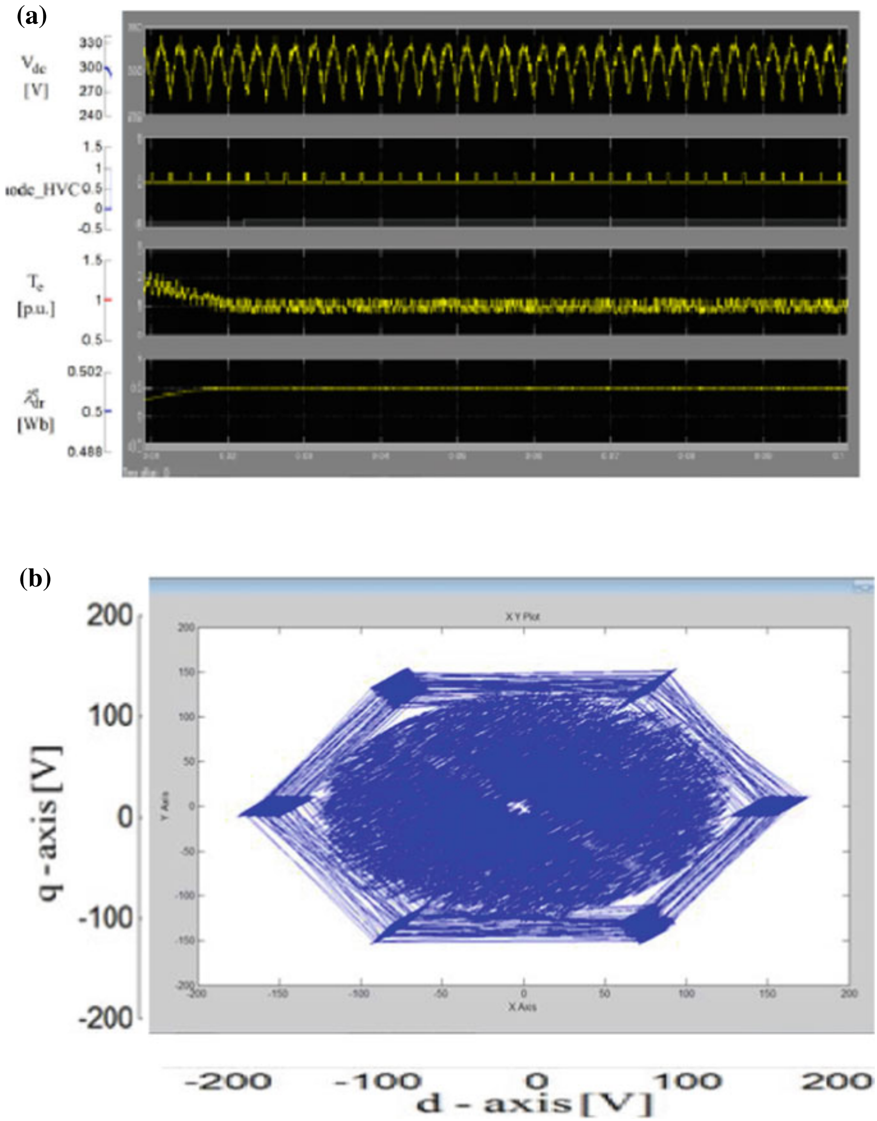

Fig. 6 **a** Simulink result with parameter 1. DC-link voltage, 2. flag signal, 3. air-gap torque, 4. rotor flux linkage; **b** *X*–*Y*-axis graph of hexagonal voltage boundary *X*-axis v_{ds}^{s*} and *Y*-axis v_{qs}^{s*}

4.2 Output Graph for DC-Link Film Capacitor

Figure 6a, b shows the result of the system with the electrolytic capacitor. Figure 7a, b shows the proposed system with DC-link film capacitor, and 6.4 shows

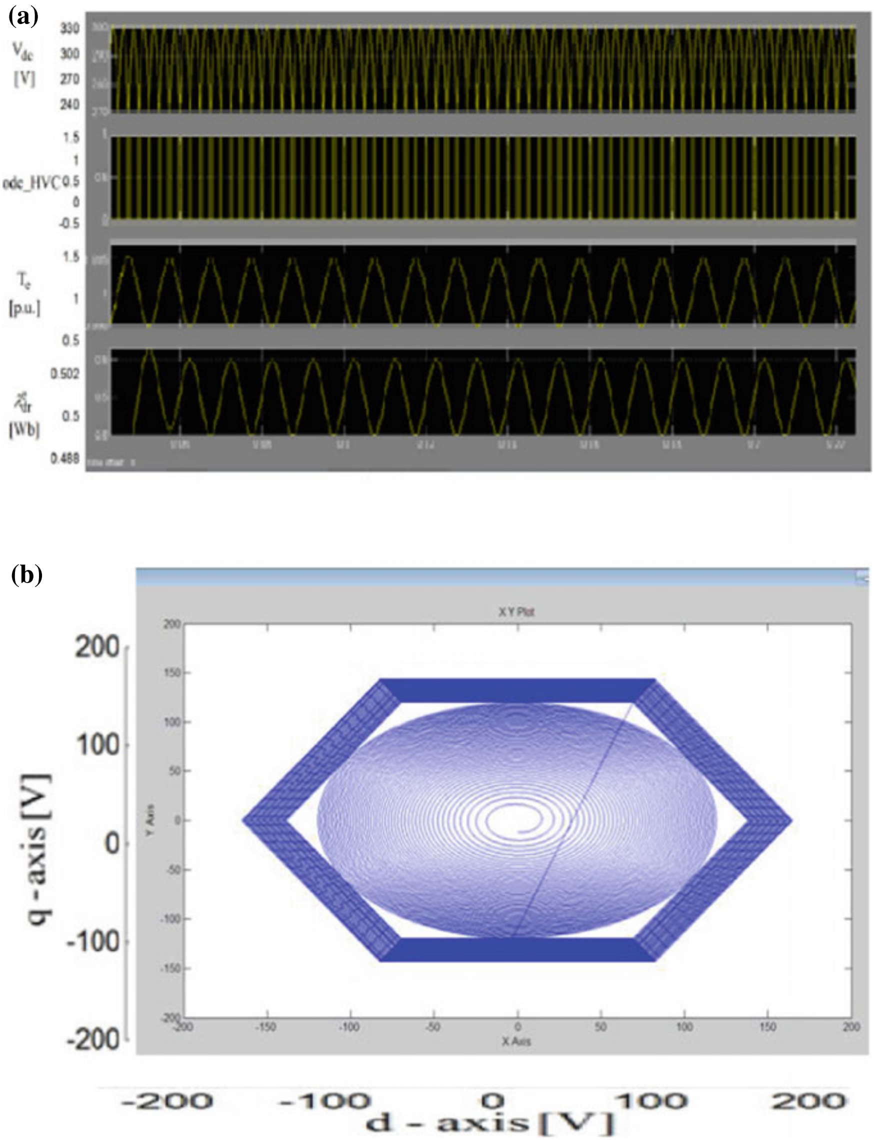

Fig. 7 **a** Simulink result with parameter 1. DC-link voltage, 2. flag signal, 3. air-gap torque, 4. rotor flux linkage **b** *X*–*Y*-axis graph of hexagonal voltage boundary *X*-axis v_{ds}^{s*} and *Y*-axis v_{qs}^{s*}

the result of the same. The resulting figure clearly shows the difference between the results by using the electrolytic capacitor.

5 Conclusion

This paper gives analytical solution leading to the dynamic voltage modification at each time step with respect to the available DC bus voltage from the results of both methods. We can say that DC-link film capacitor has advantages than electrolytic capacitor. By means, hexagonal boundary losses are reduced.

References

1. K.W. Lee, M. Kim, J. Yoon, S.B. Lee, J.Y. Yoo, Condition monitoring of DC-link electrolytic capacitors in adjustable-speed drives. IEEE Trans. Ind. Appl. **44**(5), 1606–1613 (2008)
2. M.L. Gasperi, Life prediction modeling of bus capacitors in AC variable frequency drives. IEEE Trans. Ind. Appl. **41**(6), 1430–1435 (2005)
3. A. Layhani, P. Venet, G. Grellet, P.J. Viverge, Failure prediction of electrolytic capacitors during operation of a switchmode power supply. IEEE Trans. Power Electron. **13**(6), 1199–1207 (1998)
4. A.M. Imam, T.G. Habetler, R.G. Harley, D.M. Divan, Real-time condition monitoring of the electrolytic capacitors for power electronics applications. in *Proceedings IEEE Applied Power Electronics Conference* (2007), pp. 1057–1061
5. A. Yoo, S.K. Sul, H. Kim, K.S. Kim, Flux-weakening strategy of an induction machine driven by an electrolytic-capacitor-less inverter. IEEE Trans. Ind. Appl. **47**(3), 1328–1336 (2011)
6. L. Malesani, L. Rossetto, P. Tenti, P. Tomasin, AC/DC/AC PWM converter with reduced energy storage in the DC link. IEEE Trans. Ind. Appl. **31**(2), 287–292 (1995)